Soft Matter

Accepted Manuscript

This is an *Accepted Manuscript*, which has been through the Royal Society of Chemistry peer review process and has been accepted for publication.

Accepted Manuscripts are published online shortly after acceptance, before technical editing, formatting and proof reading. Using this free service, authors can make their results available to the community, in citable form, before we publish the edited article. We will replace this *Accepted Manuscript* with the edited and formatted *Advance Article* as soon as it is available.

You can find more information about *Accepted Manuscripts* in the **Information for Authors**.

ROYAL SOCIETY OF CHEMISTRY

www.rsc.org/softmatter

Journal Name

ARTICLE TYPE

Diffusion of Eccentric Microswimmers

Debajyoti Debnath,[a] Pulak K. Ghosh,[a] Yunyun Li,[*b] Fabio Marchesoni,[b,c] and Baowen Li[d]

We model the two-dimensional diffusive dynamics of an eccentric artificial microswimmer in a highly viscous medium. We assume that the swimmer's propulsion results from an effective force applied to a center distinct from its center of mass, both centers resting on a body's axis parallel to its average self-propulsion velocity. Moreover, we allow for angular fluctuations of the velocity about the body's axis. We prove, both analytically and numerically, that the ensuing active diffusion of the swimmer is suppressed to an extent that strongly depends on the model parameters. In particular, the active diffusion constant undergoes a transition from a quadratic to a linear dependence on the self-propulsion speed, with practical consequences on the interpretation of the experimental data. Finally, we extend our model to describe the diffusion of chiral eccentric swimmers.

1 Introduction

Self-propulsion is the ability of specially designed synthetic microparticles to propel themselves by harvesting kinetic energy from an active environment[1–3]. Contrary to bacteria[4–7], self-propulsion of inorganic microswimmers is fueled by stationary *external* nonequilibrium processes, like directional "power-strokes" from catalytic chemical reactions or self-phoresis by short-scale (electric[8], thermal[9] or chemical[10]) gradients, generated by the particles themselves, by virtue of some built-in functional asymmetry[11].

The simplest and, possibly, best established model of self-propulsion for artificial swimmers diffusing in an equilibrium suspension fluid at rest, is encoded by the two-dimensional (2D) Langevin equations (LE)[12–16]

$$\dot{x} = v_0\cos\phi + \sqrt{D_0}\,\xi_x(t),$$
$$\dot{y} = v_0\sin\phi + \sqrt{D_0}\,\xi_y(t),$$
$$\dot{\phi} = \sqrt{D_\phi}\,\xi_\phi(t), \tag{1}$$

where $\mathbf{r} = (x,y)$ are the coordinates of spherically symmetric (or pointlike) swimmer in the plane, ϕ is the angle between the x axis and its self-propulsion velocity vector of *constant* modulus v_0.

[a] Department of Chemistry, Presidency University, Kolkata 700073, India.
[b] Center for Phononics and Thermal Energy Science, School of Physics Science and Engineering, Tongji University, Shanghai 200092, People's Republic of China Fax: 86 (21)6598 6745; Tel: 86 (21)6598 1360; E-mail: yunyunli@tongji.edu.cn
[c] Dipartimento di Fisica, Università di Camerino, I-62032 Camerino, Italy
[d] Department of Mechanical Engineering, University of Colorado, Boulder, Colorado 80309, USA

The Gaussian noises $\xi_i(t)$, with $i = x,y,\phi$, are assumed to be zero-mean valued and delta-correlated, that is $\langle\xi_i(t)\xi_j(0)\rangle = 2\delta_{ij}\delta(t)$; D_ϕ plays the role of an orientational diffusion constant, whose inverse, τ_ϕ, quantifies the temporal persistency of the ensuing *isotropic* Brownian motion. Indeed, for long observation times t, with $t \gg \tau_\phi$, the asymptotic law $\lim_{t\to\infty}\langle\mathbf{r}^2(t)\rangle = 4Dt$[17], defines an effective diffusion constant $D = D_0 + D_s$. Here, D_0 is due to the environmental thermal fluctuations, while $D_s = v_0^2/2D_\phi$ is the (typically) much larger self-propulsion term, which depends on the activation properties of the swimmer in the suspension fluid. Note that restricting our analysis to the 2D case affords substantial algebraic simplifications without prejudice of the general validity of our conclusions.

In the standard model of Eq. (1) two main assumptions are implicit: (1) The self-propulsion velocity v_0 is constant and, most importantly, oriented along a certain symmetry axis of the particle, like the longitudinal axis in the case of an active nanorod with one active tip[8], or the diameter perpendicular to the equatorial plane dividing the two faces of a spherical Janus particle[2,3], as sketched in Fig. 1; (2) The center of the force responsible for the swimmer's propulsion coincides with the swimmer's center of mass. Under these conditions, the only effect of the angular dynamics described by the process $\phi(t)$ is to make the swimmer change direction, so that its active motion, intrinsically ballistic according to the first two LEs (1), turns into a diffusive one with persistence time τ_ϕ.

Clearly, both assumptions, although adequate to model a generic active Brownian particle, fail to reproduce specific features of the swimmer's propulsion mechanism that may well impact its diffusive properties. In particular, the finite spatio-temporal scales governing the propulsion mechanism suggest that

Fig. 1 (Color online) Swimmer's self-propulsion mechanism: O and P are respectively the center of mass and the center of force of a spherical Janus particle. $\mathbf{v}_0$ represents the instantaneous self-propulsion velocity vector; ϕ and ψ denote the angle between the OP axis and, respectively, the x axis and $\mathbf{v}_0$. The average direction of $\vec{v}_0$ is oriented parallel to OP.

changes in the orientation of the self-propulsion velocity do not necessarily imply body's rotations[18–20]. As a consequence, the vector $\mathbf{v}_0$ ought to be allowed to fluctuate around its average direction (the body's axis of coordinate ϕ) with non-zero relaxation time and variance. On the other hand, the self-propulsion speed, v_0, results from the "effective" force[21] exerted by the suspension fluid on the active surface of the particle at low Reynolds numbers (overdamped regime). Contrary to the case of an externally applied driving force, the center of such a force does not necessarily coincide with the particle's center of mass. In general, the two centers are separated by a finite distance, which depends on the swimmer's composition, geometry and surface functionalization. For simplicity, in Fig. 1 we assume that both centers rest on the axis of coordinate ϕ.

In this paper we combine analytical arguments and numerical simulations to prove that upon relaxing assumption (1) alone, the angular reorientation of the swimmer occurs on a shorter time scale. Since the active diffusion constant, $D - D_0$, is proportional to such a characteristic time, the ensuing diffusion process gets suppressed. Eccentric swimmers, where, in violation of assumption (2), the center of force and center of mass are a distance apart, exhibit an even more intriguing dependence on the system parameters. On increasing v_0 their active diffusion constant grows from quadratic to linear in v_0, the transition being often signaled by a plateau. Moreover, eccentricity leads to an overall suppression of the swimmer's active diffusion.

To appreciate the practical consequence of these conclusions, we remind that the quantities v_0, D_0 and D are experimentally accessible, so that the rotational rate D_ϕ in Eq. (1) is estimated through the identity $D_s = v_0^2/2D_\phi$. This means that the experimental data available for D_ϕ are based on indirect measurements. However, we show here that such estimates are sensitive to swimmer's propulsion parameters, like the eccentricity and the fluctuations of the propulsion velocity in the body frame, which are usually neglected. All this supports the suggestion[18,19] that modeling swimmer propulsion mechanisms may prove a more complicated task than anticipated. On the other hand, a more refined analysis of active diffusion is expected to find concrete implementation in such technological tasks, like the design and operation of micro-robots and other micro-devices powered by active swimmers, or the control of artificial micro-swimmer transport for biomedical applications[8].

The contents of this paper is organized as follows. In Sec. 2 we present a simple model that accounts for the angular fluctuation of the self-propulsion velocity in the body frame of an eccentric microswimmer. By such a model we introduce two additional parameters besides the swimmer's eccentricity, namely the relaxation rate and variance of the angle ψ between the instantaneous self-propulsion velocity vector and its time average. In Sec 3 we first discuss the diffusion dynamics of non-eccentric swimmers for different values of the parameters that characterize the stochastic dynamics of $\psi(t)$. In Sec. 4 we consider the more general case of swimmers with increasing eccentricity and investigate the conditions under which their active diffusion constant undergoes a transition from a quadratic to a linear function of v_0. In Sec. 5 we model the chiral behavior of an eccentric swimmer by imposing a persistent misalignment between its self-propulsion velocity and the axis through its two centers. Finally, in Sec. 6 we discuss the phenomenological consequences of our results.

2 The model

The self-propulsion model we propose is illustrated by the sketch of Fig. 1. We assume that the center of force, P, and the center of mass, O, rest on a swimmer's symmetry axis. The instantaneous self-propulsion velocity is oriented at an angle ψ with respect to the axis OP and fluctuates around it, with constant modulus, v_0, and finite relaxation rate, κ_ψ, and variance, $\langle \psi^2 \rangle$. For convenience, $\psi(t)$ is thus described by a stationary Ornstein-Uhlenbeck process[17]. Due to the propulsion force applied in P, the overdamped swimmer tends to rotate around its center of mass, subject to a torque with ψ-dependent angular frequency, $-\alpha v_0 \sin \psi$, and moment of inertia $I_\alpha = I_\alpha(\alpha)$ with $I_\alpha(0) = 1$. The latest equality amounts to scaling all lengths by an appropriate characteristic length l, that is, $x \to x/l$, $y \to y/l$, so that α represents the dimensionless OP distance. The dependence of the rescaled moment of inertia, I_α, on the swimmer's eccentricity is left unspecified. We only argue that it ought to be a growing, even function of α. The resulting swimmer's dynamics is thus modeled through the set of four LEs,

$$\dot{x} = v_0 \cos(\phi + \psi) + \sqrt{D_0}\, \xi_x(t),$$

$$\dot{y} = v_0 \sin(\phi + \psi) + \sqrt{D_0}\, \xi_y(t),$$

$$\dot{\phi} = -v_0(\alpha/I_\alpha) \sin \psi + \sqrt{D_\phi/I_\alpha}\, \xi_\phi(t),$$

$$\dot{\psi} = -\kappa_\psi \psi + \sqrt{D_\psi}\, \xi_\psi(t), \tag{2}$$
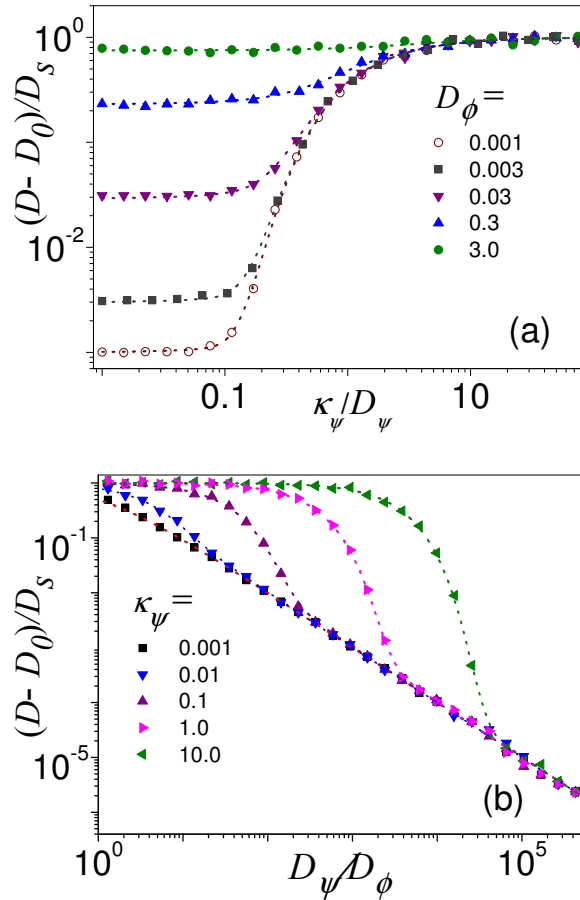
Fig. 2 (Color online) Diffusion constant of a non-eccentric swimmer with $\alpha = 0$: (a) D vs. κ_ψ for $D_\psi = 1$ and different values of D_ϕ (legend), and (b) D vs. D_ψ for $D_\phi = 0.003$ and different values of κ_ψ (legend). In both panels $v_0 = 1$, $D_0 = 0.01$. The dashed curves in (a) and (b) are the analytical predictions of Eq. (7).

where x and y are the coordinates of O and all noises are statistically uncorrelated and defined as in Eq. (1). We recall[17] that the process $\psi(t)$ is Gaussian with zero mean, autocorrelation function

$$\langle \psi(t)\psi(0)\rangle = \langle \psi^2 \rangle e^{-\kappa_\psi t}, \tag{3}$$

and variance $\langle \psi^2 \rangle = D_\psi/\kappa_\psi$. For $D_\psi/\kappa_\psi \ll 1$, the velocity fluctuations in the body frame are suppressed and the standard model of Eq. (1) is recovered. Since the LE for ψ is invariant under the transformation $\psi \to -\psi$, it follows immediately that the LE for ϕ is invariant under the simultaneous transformations $(\alpha, \psi) \to (-\alpha, -\psi)$ and, therefore, the swimmer's diffusion is insensitive to the sign of α. For this reason, the eccentricity parameter can be restricted to nonnegative values, $\alpha \geq 0$, without loss of generality.

We remark that the swimmer's eccentricity was implemented here for the possibly oversimplified case of a spherically symmetric and perfectly isotropic particle. Realistic eccentric swimmers are more likely anisotropic, too, typical examples being the active colloidal particles of arbitrary geometries (L-shaped, ellipsoidal, rod-like, etc) widely investigated in the current literature. Extending our model to account for non-spherical swimmers would

require implementing the tedious formalism of anisotropic mobility and diffusion tensors, as discussed for instance in Refs.[22,23]. Of course, such an approach would be more exhaustive, but has the drawback of obscuring the role of eccentricity by adding unnecessary details to the model.

The stochastic differential Eqs. (2) were numerically integrated by means of a standard Euler-Maruyama scheme[24]. The stochastic averages were taken over an ensemble of trajectories with random initial swimmer orientation, i.e., a uniform distribution with $\phi(0) \in [0, 2\pi]$ for ϕ, and a Gaussian distribution with variance D_ψ/κ_ψ for ψ. The additional relaxation rates, κ_ψ and D_ψ, do not alter the well-established normal diffusion law, $\lim_{t\to\infty}\langle \mathbf{r}^2(t)\rangle = 4Dt$, mentioned in Sec. 1, but rather allow the spatial diffusion constant, D, to be tuned.

In the remaining sections we will thus compare the output of our numerical simulations with analytical predictions for the diffusivity, D, either exact or approximate, depending on the choice of the model parameters. To this purpose we had recourse to Kubo's formula[16,17,25,26]

$$D = \int_0^\infty \langle \dot{x}(t)\dot{x}(0)\rangle dt = D_0 + \int_0^\infty C(t)dt, \tag{4}$$

with $C(t) = v_0^2 \langle \cos[\phi(t) + \psi(t)]\cos[\phi(0) + \psi(0)]\rangle$. Note that our model is isotropic so that D can equivalently be computed along either orthogonal axis in the plane. We also notice that the diffusion contribution from the translational (thermal) fluctuations of the coordinates x and y boils down to the additive term D_0 in the second identity of Eq. (4). Therefore, we will focus below our attention on the active term of the diffusion constant, $D - D_0$, and how much it deviates from the predicted value, $D_s = v_0^2/2D_\phi$, of the standard model of Eq. (1).

3 Diffusion of non-eccentric swimmers

We start our analysis with the exactly integrable case of a non-eccentric swimmer. At $\alpha = 0$ the LEs for ϕ and ψ decouple, so that $\phi(t)$, too, is Gaussian. As a consequence, the angular autocorrelation function $C(t)$ factorizes, namely $C(t) = v_0^2 \langle \cos \phi(t) \cos \phi(0)\rangle [\langle \cos \psi(t) \cos \psi(0)\rangle + \langle \sin \psi(t) \sin \psi(0)\rangle]$. Due to the Gaussian statistics of $\phi(t)$ and $\psi(t)$, we easily derive the useful identities

$$\langle \cos \phi(t) \cos \phi(0)\rangle = (1/2)e^{-\langle \Delta\phi^2(t)\rangle/2},$$

$$\langle \cos \psi(t) \cos \psi(0)\rangle = e^{-\langle \psi^2 \rangle}\cosh\langle \psi(t)\psi(0)\rangle,$$

$$\langle \sin \psi(t) \sin \psi(0)\rangle = e^{-\langle \psi^2 \rangle}\sinh\langle \psi(t)\psi(0)\rangle, \tag{5}$$

where $\langle \Delta\phi^2(t)\rangle = 2D_\phi t$ and $\langle \psi(t)\psi(0)\rangle$ is given in Eq. (3).

On inserting these equalities in the factorized expression for $C(t)$ we arrive at

$$C(t) = (v_0^2/2)e^{-\frac{D_\psi}{\kappa_\psi}} \exp\left[-D_\phi t + \frac{D_\psi}{\kappa_\psi}e^{-\kappa_\psi t}\right], \tag{6}$$

Kubo's integral can be calculated explicitly in powers of D_ψ/κ_ψ,

namely[27]

$$D - D_0 = D_s e^{-D_\psi/\kappa_\psi} \sum_{m=0}^{\infty} \frac{1}{m!} \frac{(D_\psi/\kappa_\psi)^{m+1}}{m(D_\psi/D_\phi) + (D_\psi/\kappa_\psi)}$$

$$= D_s \Gamma\left(1 + \frac{D_\phi}{\kappa_\psi}\right) \sum_{m=0}^{\infty} \frac{(-D_\psi/\kappa_\psi)^m}{\Gamma(m+1+D_\phi/\kappa_\psi)}, \qquad (7)$$

where $\Gamma(x)$ denotes a gamma function. This expression closely reproduces the simulation data plotted in Fig. 2 for different values of the model parameters.

A few limiting regimes of Eq. (7) can be evaluated explicitly. When the relaxation rate of the propulsion angular fluctuations in the body frame is much smaller than the body's rotational diffusion constant, that is for $D_\phi/\kappa_\psi \gg 1$, making use of the approximation[27]

$$\lim_{x \to \infty} \frac{\Gamma(x+a)}{\Gamma(x)} = e^{a \ln x}$$

in the second identity of Eq. (7), yields

$$D - D_0 = D_s \frac{D_\phi}{D_\phi + D_\psi}. \qquad (8)$$

The emergence of this decay law of the active diffusions constant is apparent in Fig. 2(b) for small κ_ψ. In the opposite and more realistic case of fast relaxing and small amplitude angular fluctuations of the self-propulsion velocity, that is for $D_\phi/\kappa_\psi \ll 1$ and $D_\psi/\kappa_\psi \ll 1$, from the first identity in Eq. (7) follows immediately that

$$D - D_0 = D_s e^{-D_\psi/\kappa_\psi}. \qquad (9)$$

In any case, the active diffusion constant, $D - D_0$, gets suppressed by raising the relaxation time of the self-propulsion fluctuations in the body frame. The physical interpretation of this effect is straightforward: weakening the restoring constant κ_ψ favors the spatial reorientation of the swimmer's kinematic velocity and, correspondingly, the suppression of its spatial diffusivity[28].

4   Diffusion of eccentric swimmers

The diffusion of eccentric swimmers exhibits a much richer phenomenology. Its most intriguing properties are illustrated in Fig. 3, where we plotted the active diffusion constant, $D - D_0$, versus the self-propulsion speed for different values of the dynamical parameters. Prominent features of the curves $D(v_0)$ are:

(i) The transition from a quadratic to a linear dependence on v_0. The linear regime for high values of v_0 is peculiar of eccentric swimmers and disappears at $\alpha = 0$, panel (a);

(ii) The two regimes are separated by a plateau for intermediate v_0 values, which grows wider on increasing the eccentricity, panel (a);

(iii) On a closer inspection, two distinct quadratic regimes are distinguishable, respectively, for $D_\psi/\kappa_\psi \ll 1$ and $D_\psi/\kappa_\psi \gg 1$, panels (b) and (c), transitions between them occurring on raising v_0 for appropriate choices of the model parameters, panel (c);

(iv) Decreasing the rotational diffusion constant, D_ϕ, tends to suppress the quadratic regime, panel (d), by widening the plateau.

Kubo's formula provides a simple quantitative interpretation of
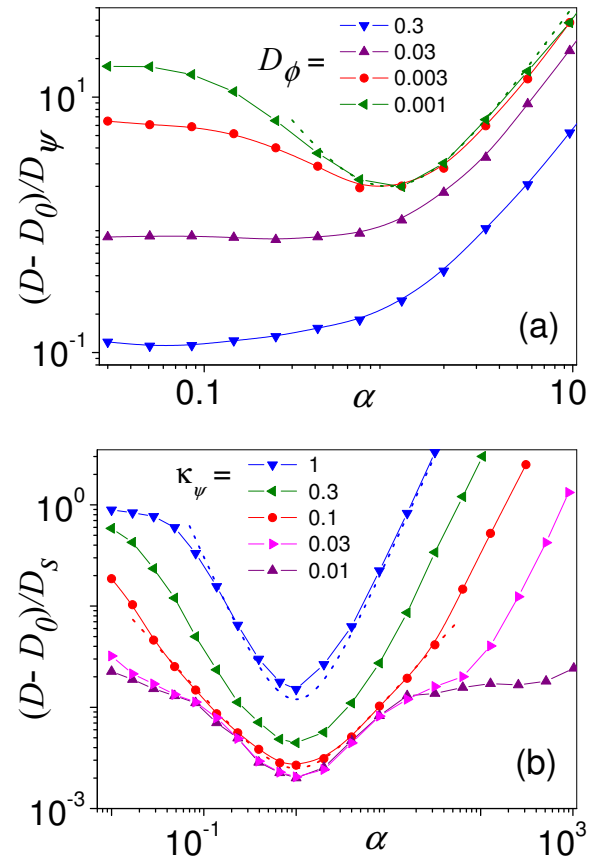
Fig. 4 (Color online) Active diffusion constant versus eccentricity, $D - D_0$ vs. α for: (a) $v_0 = 0.1$, $\kappa_\psi = 0.1$ and different D_ϕ; (b) $v_0 = 3.0$, $D_\phi = 0.003$ and different κ_ψ. In both panels $D_0 = 0.01$ and $D_\psi = 0.1$. The dashed curves represent our analytical predictions: (a) the plateau of Eq. (13); (b) the plateau of Eq. (13) for the largest κ_ψ, and the linear regime of Eq. (15) with $\kappa_\psi = D_\psi = 0.1$ (which also coincides with the non-Gaussian estimate reported in the text).

these results. Computing the angular autocorrelation function, $C(t)$, is no easy task, as for $\alpha > 0$ the variables ϕ and ψ are coupled. However, in the physically relevant regime of small ψ fluctuations, $D_\psi/\kappa_\psi \ll 1$, the approximation $\sin \psi \sim \psi$ allows us to treat $\phi(t)$ in Eq. (2) as a Gaussian process. Accordingly, the calculation of D follows immediately the procedure of Sec. 3 with the only difference that here

$$\langle \Delta\phi^2(t) \rangle = 2[D_\phi/I_\alpha]t + \qquad (10)$$

$$(\alpha v_0/I_\alpha)^2 e^{-\langle \psi^2 \rangle} \int_0^t \int_0^t \sinh\langle \psi(s)\psi(s') \rangle ds ds',$$

with the restriction $D_\psi/\kappa_\psi \ll 1$. [The second term on the r.h.s. of Eq. (10) has been obtained with the help of the third identity of Eq. (5).] When trying to integrate $C(t)$ in Kubo's formula, one singles out a few parameter domains where the task can be carried out analytically:

(1) Plateau regime. For large enough κ_ψ and v_0, such that both inequalities $D_\psi/\kappa_\psi \ll 1$ and

$$\frac{1}{I_\alpha} \frac{D_\phi}{D_\psi} + \left(\frac{v_0}{\kappa_\psi}\right)^2 \left(\frac{\alpha}{I_\alpha}\right)^2 \ll \frac{\kappa_\psi}{D_\psi}, \qquad (11)$$
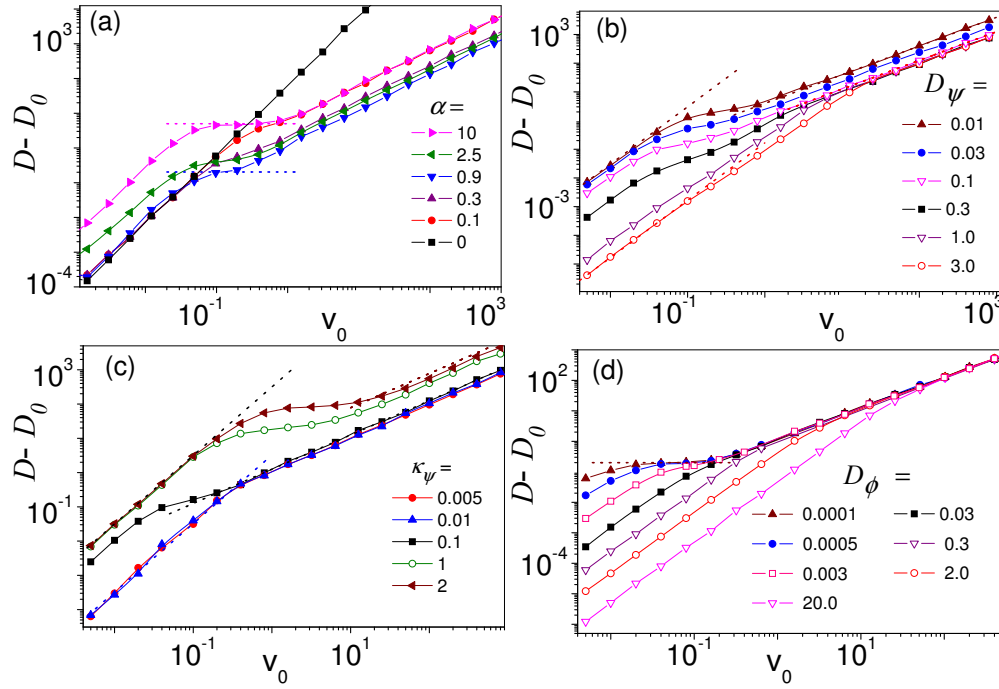
Fig. 3 (Color online) Diffusion constant versus propulsion speed for an eccentric swimmer with $D_0 = 0.01$ and $\alpha > 0$: D vs. v_0 for (a) for $\kappa_\psi = 0.1$, $D_\psi = 0.1$, $D_\phi = 0.003$ and different α; (b) $\kappa_\psi = 0.1$, $\alpha = 1.0$, $D_\phi = 0.003$ and different D_ψ; (c) $D_\phi = 0.003$, $D_\psi = 0.1$, $\alpha = 1.0$, and different κ_ψ; (d) $\kappa_\psi = 0.1$, $D_\psi = 0.1$, $\alpha = 1.0$, and different D_ϕ (see legends). All quantities plotted here have the dimensions of $[t^{-1}]$, and are expressed in units of the model Eqs. (2). The dashed curves in (a) and (b) are our analytical predictions from Sec. 4: (a) plateaus, Eq. (13) for $\alpha = 10$ (top) and 0.9 (bottom); (b)-(c) quadratic, Eq. (18), and linear regime, Eq. (15), respectively for $D_\psi = 0.01$ and $\kappa_\psi = 2.0$ (top data sets); quadratic, Eq. (19), and non-Gaussian linear regime (see text), respectively for $D_\psi = 3.0$ and $\kappa_\psi = 0.005$ (bottom data sets); (d) plateau, Eq. (13).

hold, $C(t)$ in Kubo's integral can be approximated by

$$C(t) \simeq \frac{v_0^2}{2} e^{-\frac{D_\psi}{\kappa_\psi}} \tag{12}$$

$$\times \exp\left[-\frac{D_\phi}{I_\alpha}t - e^{-\frac{D_\psi}{\kappa_\psi}}\left(\frac{v_0}{\kappa_\psi}\right)^2\left(\frac{\alpha}{I_\alpha}\right)^2 D_\psi t\right],$$

hence

$$D - D_0 = \frac{D_s I_\alpha}{e^{D_\psi/\kappa_\psi} + (D_\psi/D_\phi)(v_0/\kappa_\psi)^2(\alpha^2/I_\alpha)}$$

$$\simeq \frac{\kappa_\psi^2}{2D_\psi}\left(\frac{I_\alpha}{\alpha}\right)^2, \tag{13}$$

the second equality holding only for $(v_0/\kappa_\psi)^2 \gg D_\phi/D_\psi$. This analytical expression closely reproduces the plateaus of the curves $D(v_0)$ in Fig. 3 for the largest α and v_0, and the smallest D_ϕ values plotted there.

(2) Linear regime. On increasing v_0 beyond the plateau range, the inequality (11) eventually fails. In such a limit, and more precisely for $v_0/\kappa_\psi \gg I_\alpha/\alpha$, the Kubo's integral is dominated by the short-time decay of $\langle \Delta\phi^2(t)\rangle$, Eq. (10), so that

$$C(t) \simeq \frac{v_0^2}{2}\exp\left[-\left(\frac{D_\psi}{\kappa_\psi}\right)\left(\frac{v_0}{\kappa_\psi}\right)^2\left(\frac{\alpha}{I_\alpha}\right)^2\frac{(\kappa_\psi t)^2}{2}\right], \tag{14}$$

which, after integration, yields

$$D - D_0 = \frac{v_0}{2}\sqrt{\frac{\pi}{2}}\frac{I_\alpha}{\alpha}\sqrt{\frac{\kappa_\psi}{D_\psi}}. \tag{15}$$

In the case of large ψ fluctuations, $D_\psi/\kappa_\psi \gg 1$, the Gaussian approximation of Eq. (10) is no longer tenable. Nevertheless, one can prove (not shown here) that Eq. (15) still applies upon replacing the factor $\sqrt{\kappa_\psi/D_\psi}$ with 1.

(3) Quadratic regimes. In Fig. 3 the quadratic branches of the $D(v_0)$ curves are always detectable as long as we move to small enough v_0. Indeed, as $v_0 \to 0$, the integrand $C(t)$ in Kubo's formula can be approximated to

$$C(t) \simeq (v_0^2/2)e^{-D_\psi/\kappa_\psi}e^{-D_\phi t/I_\alpha}, \tag{16}$$

for $\kappa_\psi \gg D_\phi/I_\alpha$, and

$$C(t) \simeq (v_0^2/2)e^{-[D_\phi/I_\alpha + D_\psi]t}, \tag{17}$$

for $\kappa_\psi \ll D_\phi/I_\alpha$. Accordingly, the active diffusion constant tends, respectively, to

$$D - D_0 = D_s I_\alpha e^{-D_\psi/\kappa_\psi}, \tag{18}$$

and

$$D - D_0 = \frac{D_s I_\alpha}{I_\alpha D_\psi/D_\phi + 1}, \tag{19}$$

where we remind that $D_s = v_0^2/2D_\phi$. Since $I(0) = 1$, the limits
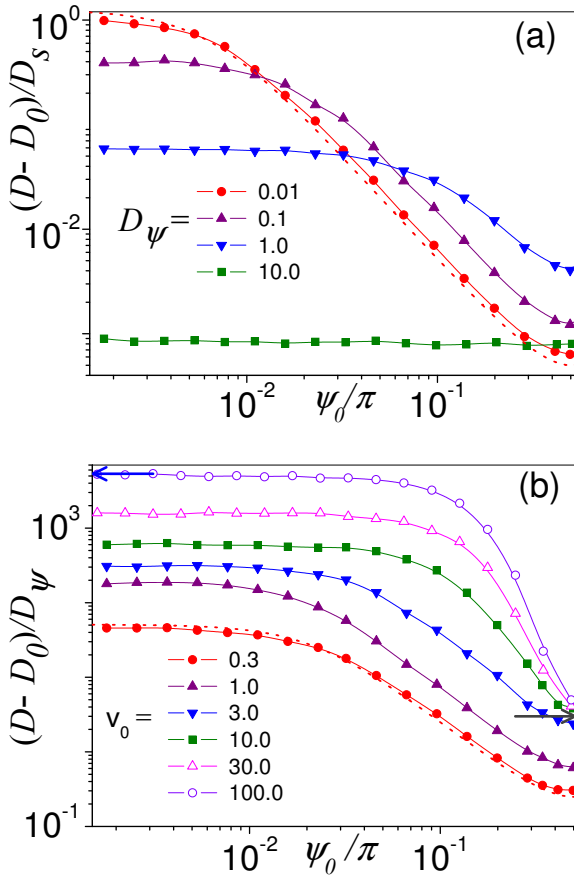
Fig. 5 (Color online) Active diffusion constant of a chiral eccentric swimmer, $D - D_0$ vs. ψ_0 for: (a) $v_0 = 1.0$, and different D_ψ; (b) $D_\psi = 0.1$ and different v_0. In both panels $D_0 = 0.01$, $D_\phi = 0.01$, $\kappa_\psi = 1.0$ and $\alpha = 0.5$. The dashed curves in (a) and (b) are the analytical predictions of Eq. (23) with $\bar{D}$ given in Eq. (18); the arrows in (b) indicate the predicted minima accumulation point of Eq. (25), bottom right, and the linear regime estimate of Eq. (15) for $\psi_0 = 0$, top left.

$\alpha \to 0$ of Eqs. (18) and (19) coincide with the corresponding diffusion constants of Eqs. (9) and (8) for a non-eccentric swimmer. Both quadratic behaviors of the $D(v_0)$ curves are clearly distinguishable in Fig. 3(c). One curve in particular exhibits a crossover between the quadratic laws of Eqs. (18) and (19) for $\kappa_\psi/D_\psi \sim (\alpha/I_\alpha)(v_0/\kappa_\psi)$, see inequality (11) for $D_\phi \ll D_\psi$. Indeed, such a crossover may set in before the transition to the linear regime takes place.

Transitions between the diffusive regimes detailed above were obtained in Fig. 4 by varying the swimmer's eccentricity, α, at constant self-propulsion speed, v_0. We used here α as a free parameter with $0 \leq \alpha < \infty$ to numerically test the analytical results of the section. For mere geometric reasons, realistic values of α ought to be quite small, that is, $0 \leq \alpha \ll 1$. In our simulations we set $I_\alpha = 1 + \alpha^2$, so that the ratio I_α/α has a minimum equal to 2 for $\alpha = 1$. We plotted the active diffusion constant, $D - D_0$, versus α both at low, panel (a), and large v_0, panel (b).

In Fig. 4(a) the condition $v_0/\kappa_\psi \ll I_\alpha/\alpha$ holds for any α, so that the only detectable transition is from the quadratic to the plateau regime. In the limit of vanishingly small α both quadratic regimes of Eqs. (18) and (19) were recovered, respectively for the lowest

and the largest D_ϕ values, in good agreement with the analytical predictions. For appropriately large α values the inequality (11) holds irrespective of the remaining model parameters. In view of the discussion above, this implies that the plateau regime eventually sets in, but no more regime changes are expected on further increasing α. In both panels of Fig. 4 the plateau regime corresponds to the quadratic branches of the $D(\alpha)$ curves, see Eq. (13).

In Fig. 4(b) v_0 was chosen large enough to satisfy the condition (11) with $v_0/\kappa_\psi \gg I_\alpha/\alpha$, required to detect the linear diffusive regime of Eq. (15). Of course that was only possible for a certain neighborhood of $\alpha = 1$, where I_α/α and, therefore the $D(\alpha)$ curves hit a minimum. On increasing α, I_α/α grows larger until the linear regime condition fails and a change in the diffusive regime must occur. At large κ_ψ, $D_\psi/\kappa_\psi \ll 1$, the expected transition toward the plateau regime, proportional to α^2, is clearly detectable. At low κ_ψ, $D_\psi/\kappa_\psi \gg 1$, the active diffusion curves first approach the quadratic regime of Eq. (19), which is almost insensitive to α, and then turn upward quadratically for exceedingly large values of α, thus signaling a final transition to the plateau regime.

5 Diffusion of chiral eccentric swimmers

We extend now our analysis to discuss the diffusion of eccentric circle swimmers [14]. We assume, for instance, that the self-propulsion velocity in the body frame is directed in average at an angle ψ_0 with respect to the axis OP. This means that an overdamped swimmer is subjected to an effective torque with nonzero mean angular frequency, $\Omega_\psi = -[\alpha/I_\alpha]\langle \sin \psi \rangle \neq 0$. Its trajectory then consists of a random sequence of circular arcs the particle traces counterclockwise for $\Omega_\psi > 0$, or clockwise for for $\Omega_\psi < 0$, termed, respectively, positive and negative chiral trajectories. Accordingly, the forth LE of the set of model Eqs. (2) is rewritten as

$$\dot{\psi} = -\kappa_\psi(\psi - \psi_0) + \sqrt{D_\psi}\,\xi_\psi(t), \qquad (20)$$

where $\psi_0 \in [-\pi, \pi]$. On inspecting Eqs. (2) and (20) one concludes immediately that changing the sign of ψ_0 is equivalent to transforming the spatial coordinates as $(x, y, \phi) \to (x, -y, -\phi)$, so that the swimmer's chirality does change sign, but its active diffusion stays the same, or, stated otherwise, D is a function of $|\Omega_\psi|$.

An intrinsic rotational torque on a floating swimmer can be either the accidental result of a fabrication defect or a desired effect obtained, e.g., by bending an active nanorod [29,30]. In the current literature [14,16,21,31] swimmer's chirality is modeled by adding an *ad hoc* bias, Ω, to the LE for ϕ, namely, $\dot{\phi} = \Omega + \sqrt{D_\phi}\,\xi_\phi(t)$. In the present model the torque frequency emerges as a dynamical effect due to the misalignment of the propulsion velocity with the OP axis of the swimmer. Since the biased process $\psi(t)$ in Eq. (20) is Gaussian, an explicit analytical expression for the average torque frequency is readily derived, that is

$$\Omega_\psi = -\frac{v_0 \alpha}{I_\alpha} \sin \psi_0\, e^{-D_\psi/2\kappa_\psi}. \qquad (21)$$

As already stated in the literature, chirality suppresses diffusion. This conclusion applies to eccentric swimmers, too, as illustrated

in Fig. 5. Note that $|\Omega_\psi|$ is a monotonically increasing function of ψ_0 for $0 < \psi_0 < \pi/2$, so that we expect D to have a maximum at $\psi_0 = 0$ and a minimum at $\psi_0 = \pi/2$, with mirror symmetry around both points, i.e., $D(-\psi_0) = D(\psi_0)$ and $D(-\psi_0 + \pi/2) = D(\psi_0 - \pi/2)$. For this reason, the simulation curves for D as a function of ψ_0 in Fig. 5 are plotted in the reduced range $\psi_0 \in [0, \pi/2]$.

Calculating the spatial diffusion of a chiral swimmer from Kubo's formula is still an affordable task, though rather tedious. In Gaussian approximation, $D_\psi/\kappa_\psi \ll 1$, the difference between the model for chiral and non-chiral swimmers boils down to replacing

$$-\frac{\alpha}{I_\alpha}\sin\psi \to \Omega_\psi - \frac{\alpha}{I_\alpha}\cos\psi_0\sin\psi,$$

in the LE (2) for the rotational coordinate ϕ. The corresponding angular autocorrelation function reads [16]

$$C(t) \simeq \frac{v_0^2}{2}\cos(\Omega_\psi t)e^{-\frac{D_\psi}{\kappa_\psi}(1-e^{-\kappa_\psi t})} \tag{22}$$

$$\times\quad \exp\left[-\frac{D_\phi}{I_\alpha}t - \cos^2\psi_0 e^{-\frac{D_\psi}{\kappa_\psi}}\left(\frac{v_0}{\kappa_\psi}\right)^2\left(\frac{\alpha}{I_\alpha}\right)^2 D_\psi t\right],$$

with Ω_ψ given in Eq. (21). Kubo's integral is worthy to be calculated analytically to explain a few interesting features of the $D(\psi_0)$ curves of Fig. 5:

(i) *Low chirality limit, $\psi_0 \to 0$.* The $C(t)$ of Eq. (22) tends to that of Eq. (16) for low v_0, and Eq. (14) for large v_0. Accordingly, in Fig. 5(b) the horizontal plateaus at low ψ_0 shift upward with v_0, retracing the crossover from the quadratic to the linear regime shown in Fig. 3 for $\psi_0 = 0$;

(ii) *Quadratic regime.* For conveniently small v_0 values, the term proportional to $\cos\psi_0$ in the exponential function of Eq. (22) can be neglected, so that for $D_\psi/\kappa_\psi \ll 1$ the two limits of Eqs. (16) and (17) are recovered, depending on the ratio κ_ψ/D_ϕ. Kubo's formula for the active diffusion constant yields

$$D - D_0 = \frac{\bar{D}}{1 + (I_\alpha\Omega_\psi/D_\phi)^2}, \tag{23}$$

where $\bar{D}$ is the corresponding value of $D - D_0$ at $\psi_0 = 0$, see Eq. (18) or (19).

(iii) *Linear regime at $\psi_0 = \pi/2$.* In Fig. 5(b) the $D(\psi_0)$ curves for large v_0 tend to approach the same minimum value at $\psi_0 = \pi/2$. This effect can be explained by noticing that at $\psi_0 = \pi/2$ the term proportional to $\cos\psi_0$ in $C(t)$ vanishes and, moreover, in the linear regime the condition $\kappa_\psi \ll \Omega_\psi$ can be achieved for any finite κ_ψ (with $D_\psi/\kappa_\psi \ll 1$) by suitably raising v_0. Under these conditions, Kubo's integral can be carried out analytically by approximating

$$C(t) \simeq (v_0^2/2)\cos(\Omega_\psi t)e^{-[D_\phi/I_\alpha + D_\psi]t}, \tag{24}$$

with $\Omega_\psi = -(v_0\alpha/I_\alpha)e^{-D_\psi/2\kappa_\psi}$. The result,

$$D - D_0 = \frac{1}{2}\left(\frac{I_\alpha}{\alpha}\right)^2 D_\psi e^{D_\psi/\kappa_\psi}, \tag{25}$$

closely locates the accumulation point of the minima of the $D(\psi_0)$ curves at large v_0.

Finally, we notice that for large angular fluctuation around ψ_0,

$D_\psi/\kappa_\psi \gg 1$, the average torque frequency, Ω_ψ of Eq. (21), tends to zero, so that the chirality effect on swimmer's diffusion vanishes. This conclusion is confirmed by the curves of Fig. 5(a), plotted for increasing values of D_ψ.

A comparison of the results presented here and in Sec. 4 suggests a simple interpretation of the transition between the quadratic and linear regimes of the curves $D(v_0)$ plotted in Fig. 3. For $\psi_0 = 0$, low propulsion velocities, and (or) large relaxation rates κ_ψ, the effective torque due to the misalignment, ψ, between $\mathbf{v}_0$ and the swimmer's symmetry axis is too small to appreciably affect the diffusion process, whose diffusion constant thus retains its standard quadratic dependence on v_0. On increasing the effective torque, the swimmer eventually behaves like a chiral particle subject to an effective torque of zero mean, magnitude of the order of $(v_0\alpha/I_\alpha)\sqrt{D_\psi/\kappa_\psi}$ and, most importantly, fluctuating sign. As a consequence, its diffusion constant does get suppressed with respect to the standard model for a non-chiral particle, but not as drastically as for a chiral swimmer with constant torque, the latter being the case analyzed in Ref. [14] and here for $\psi_0 \neq 0$. The linear regime of the $D(v_0)$ curves illustrated in Sec. 4 can be therefore regarded as a combined effect of the tendency of the swimmer's diffusivity to increase with the propulsion velocity and decrease in the presence of a torque, the propulsion velocity controlling in our model both mechanisms.

6 Conclusions

We have extended the standard model for an overdamped point-like swimmer, self-propelling itself on a frictionless planar substrate, to account for possible instability effects. Due to its functional asymmetry, the center of mass and the center of the effective propulsion force acting upon the swimmer may well lie a finite distance apart, say, along its symmetry axis, like in the case of the Janus particle of Fig. 1. As a consequence, the angular fluctuations of the self-propulsion velocity vector are associated with an additional instantaneous torque. Although such a random torque has zero mean, it suffices to suppress the active diffusion of the eccentric swimmer. In particular, the active diffusion constant exhibits a transition from a quadratic to a linear dependence on the self-propulsion speed. For more asymmetric geometries, where the average self-propulsion velocity points at an angle, $\langle\psi\rangle = \psi_0 \neq 0$, with the swimmer's axis, the ensuing nonzero average torque drives the eccentric swimmer along spiraling trajectories. This generalization of the eccentric swimmer model allowed us to study the effects of chirality on active diffusion [29,30].

The results presented in this paper are of practical use for a correct analysis of the experimental data. The current estimates of the dynamical parameters v_0 and D_ϕ of the standard model, Eqs. (1), are generally extracted from the direct measurement of the active diffusion process and, in particular, from the identity $D_s = v_0^2/2D_\phi$. It is apparent from the analysis of Sec. 4 that the combination of angular fluctuations of the propulsion velocity in the body frame and swimmer's eccentricity, strongly modifies the dependence of the active diffusion constant on the swimmer's propulsion parameters. As a consequence, the current procedure employed to extract the key quantities v_0 and D_ϕ would still be

tenable, but only at sufficiently low D_s values, where, however, the experimental accuracy worsens. An experimental evaluation of the eccentricity effects may thus become advisable.

Acknowledgements

References

1 F. Schweitzer, *Brownian Agents and Active Particles*, Springer, Berlin, 2003.

2 *Janus Particle Synthesis, Self-Assembly and Applications*, ed. S. Jiang and S. Granick, RSC Publishing, Cambridge, 2012.

3 A. Walther and A. H. E. Müller, *Chem. Rev.*, 2013, **113**, 5194–5261.

4 E. M. Purcell, *Am. J. Phys.*, 1977, **45**, 3–11.

5 M. J. McBride, *Annu. Rev. Microbiol.*, 2001, **55**, 49–75.

6 H. C. Berg, *E. coli in motion*, Springer, New York, 2003.

7 J. Elgeti, R. G. Winkler and G. Gompper, *Rep. Progr. Phys.*, 2015, **78**, 056601.

8 S. Sengupta, M. E. Ibele and A. Sen, *Angew. Chem. Int. Ed.*, 2012, **51**, 8434–8445.

9 H.-R. Jiang, N. Yoshinaga and M. Sano, *Phys. Rev. Lett.*, 2010, **105**, 268302.

10 Y. Hong, N. M. K. Blackman, N. D. Kopp, A. Sen and D. Velegol, *Phys. Rev. Lett.*, 2007, **99**, 178103.

11 R. Golestanian, T. B. Liverpool and A. Ajdari, *New J. Phys.*, 2007, **9**, 126.

12 J. G. Gibbs and Y.-P. Zhao, *Appl. Phys. Lett.*, 2009, **94**, 163104.

13 J. R. Howse, R. A. L. Jones, A. J. Ryan, T. Gough, R. Vafabakhsh and R. Golestanian, *Phys. Rev. Lett.*, 2007, **99**, 048102.

14 S. van Teeffelen and H. Löwen, *Phys. Rev. E*, 2008, **78**, 020101.

15 G. Volpe, I. Buttinoni, D. Vogt, H.-J. Kümmerer and C. Bechinger, *Soft Matter*, 2011, **7**, 8810–8815.

16 X. Ao, P. Ghosh, Y. Li, G. Schmid, P. Hänggi and F. Marchesoni, *Eur. Phys. J. Special Topics*, 2014, **223**, 3227–3242.

17 C. W. Gardiner, *Handbook of Stochastic Methods*, Springer, Berlin, 1985.

18 F. Peruani and L. G. Morelli, *Phys. Rev. Lett.*, 2007, **99**, 010602.

19 R. Golestanian, T. B. Liverpool and A. Ajdari, *Phys. Rev. Lett.*, 2005, **94**, 220801.

20 R. Golestanian, *Phys. Rev. Lett.*, 2009, **102**, 188305.

21 B. ten Hagen, R. Wittkowski, D. Takagi, F. Kümmel, C. Bechinger and H. Löwen, *J. Phys.: Condens. Matter*, 2015, **27**, 194110.

22 B. ten Hagen, S. van Teeffelen and H. Löwen, *J. Phys.: Condens. Matter*, 2011, **23**, 194119.

23 S. Weitz, A. Deutsch and F. Peruani, *Phys. Rev. E*, 2015, **92**, 012322.

24 P. E. Kloeden and E. Platen, *Numerical Solution of Stochastic Differential Equations*, Springer, 1992.

25 P. K. Ghosh, Y. Li, G. Marchegiani and F. Marchesoni, *J. Chem. Phys.*, 2015, **143**,.

26 A. Nourhani, V. H. Crespi and P. E. Lammert, *Phys. Rev. E*, 2014, **90**, 062304.

27 I. S. Gradshteyn and I. M. Ryzhik, *Table of Integrals, Series, and Products*, Academic Press, 7th edn, 2007.

28 G. Costantini and F. Marchesoni, *EPL (Europhysics Letters)*, 1999, **48**, 491.

29 F. Kümmel, B. ten Hagen, R. Wittkowski, I. Buttinoni, R. Eichhorn, G. Volpe, H. Löwen and C. Bechinger, *Phys. Rev. Lett.*, 2013, **110**, 198302.

30 D. Takagi, A. B. Braunschweig, J. Zhang and M. J. Shelley, *Phys. Rev. Lett.*, 2013, **110**, 038301.

31 Y. Li, P. K. Ghosh, F. Marchesoni and B. Li, *Phys. Rev. E*, 2014, **90**, 062301.